Image Restoration via Wiener Filtering in the Frequency Domain

Hiroko Furuya
Department of Information and Computer Sciences
Faculty of Engineering, Saitama University
Shimo-Okubo 255, Sakura-ku, Saitama, 338-8570
JAPAN
furuya@sie.ics.saitama-u.ac.jp

Shintaro Eda, Testuya Shimamura
Graduate School of Science and Engineering
Saitama University
Shimo-Okubo 255, Sakura-ku, Saitama, 338-8570
JAPAN
{shintaro, shima}@sie.ics.saitama-u.ac.jp

Abstract: - In this paper, first, the performance of the Wiener filter in the frequency domain for image restoration is compared with that in the space domain on images degraded by white noise. After finding that the Wiener filter in the frequency domain is more effective than that in the space domain in an ideal case, power spectrum estimation methods for the Wiener filter in the frequency domain are discussed. Three approaches are considered; frequency band division processing (FBDP), modified FBDP and averaging high frequency components (AHFC). The performances of the Wiener filter with the three approaches for power spectrum estimation are investigated through computer simulation experiments. It is shown that the frequency domain Wiener with the modified FBDP provides a superior performance relative to that with the FBDP and AHFC.

Key–Words: Image restoration, White noise, Power spectrum estimation, Wiener filter, Frequency domain

1 Introduction

In recent years, denoising techniques have received a great deal of attention in the field of image processing [1]-[3]. There are several approaches to image denoising, which include linear filters, nonlinear filters and Fourier / Wavelet transforms [4]-[6]. Image denoising problem is equivalent to that of image restoration when blurs are not included in the noisy image.

It is known that in the case where an image is degraded by white noise, the Wiener filter is more suitable for restoration than a variety of smoothing filters such as the Gaussian, median, Kuwahara and morphological filters [7]. The Wiener filter has two types of implementation; one is the frequency domain Wiener filtering [8] and the other is the space (time) domain one [9]. These are commonly derived in the sense to minimize the mean square error (MSE) between the noisy image and desired (original) image. However, both implementations are obviously different, resulting in different performances even for an ideal case where both the original and noisy images are known.

In this paper, we first examine which is better for the frequency domain and space domain Wiener filters for the purpose of image restoration. Simulation results in an ideal case where the original image and additive noise are known a priori visualize that the Wiener filter implemented in the frequency domain is better than that in the space domain for restoration. Thus, based on this result, we set out to improve the performance of the Wiener filter implemented in the frequency domain.

It is necessary for the frequency domain Wiener filter to estimate the original image and noise power spectra from the observed noisy image in most of the cases. The performance of the Wiener filter obviously depends on these estimates. Estimation of the original image power spectrum is essentially difficult. We do not have a single method reliable and accurate for the original image power spectrum estimation. On the other hand, there exist several types of methods to estimate the noise power spectrum. The frequency band division processing (FBDP) is one of them, which was addressed recently in [10]. The FBDP was originally derived for implementing a two-dimensional (2-D) spectral subtraction method, but it is obviously applicable to the Wiener filter as well. In this paper, the FBDP is developed for estimating the original image and noise power spectra from the observed noisy image.

Unfortunately, the noise power spectrum estimation in the FBDP does not cover the low frequency region, resulting in a poor performance of the Wiener filter under severely noisy conditions. From this reason, a modified FBDP method is derived in which the accuracy of noise power spectrum estimation is improved by incorporating a low frequency estimate of the noise power spectrum.

In addition, a simple approach in which high fre-

quency components included in the noisy image are averaged is also investigated for the noise power spectrum estimation. When the noise power spectrum is obtained in this approach, the original image power spectrum is easily obtained from the noisy image power spectrum by subtracting the noise power spectrum.

In this paper, the three approaches mentioned above to the power spectrum estimation required for the frequency domain Wiener filter are investigated in a comparative fashion. A variety of images included in Standard Image Data-BAse (SIDBA) are utilized for performance evaluation. Only white noise is considered as the additive noise, but the dependency on noise for the frequency domain Wiener filter is considerably studied by changing the signal-to-noise ratio (SNR) of the noisy image.

The rest of this paper is organized as follows. Section 2 describes the two types of Wiener filter implementations and demonstrates which is more effective in an ideal situation where the original image and noise are known a priori. Section 3 discusses the power spectrum estimation of the frequency domain Wiener filter. Three estimation approaches to the original image and noise power spectra are derived in this section. Section 4 demonstrates the performances of the frequency domain Wiener filter with the three approaches of power spectrum estimation in a comparative fashion. Finally, concluding remarks are drawn in Section 5.

2 Two Types of Wiener Filtering and Performance Comparison

In this section, we describe the principle of 2-D Wiener filters in the frequency domain and in the space domain for the purpose of restoration of an image degraded by white noise. Through this paper, we assume that $d(i,j)$ and $n(i,j)$ represent the original image and additive noise, respectively. The observed degraded image $x(i,j)$ is given by

$$x(i,j) = d(i,j) + n(i,j). \qquad (1)$$

The goal is to obtain a restored image $y(i,j)$ from $x(i,j)$, in which $y(i,j)$ should be equivalent to the original image $d(i,j)$ ideally.

2.1 Wiener Filter in the Space Domain

If the output of the Wiener filter is $y(i,j)$, it is represented by

$$y(i,j) = \sum_{m=-N}^{N} \sum_{n=-N}^{N} w(m,n)x(i+m,j+n). \quad (2)$$

The weights of the Wiener filter, $w(m,n)$, can be found by minimizing

$$J = E[\{d(i,j) - y(i,j)\}^2] \qquad (3)$$

where E denotes expectation. The solution for $w(m,n)$ is obtained in a vector form as

$$\boldsymbol{w} = \boldsymbol{R}^{-1}\boldsymbol{p} \qquad (4)$$

where

$$
\begin{aligned}
\boldsymbol{w} &= \big[w(-N,-N), ..., w(-N,N), \\
&\quad w(-N+1,-N), ..., w(-N+1,N), ..., \\
&\quad w(0,0), ..., w(N,N) \big]^T \\
\boldsymbol{p} &= \big[p(-N,-N), ..., p(-N,N), p(-N+1,-N), \\
&\quad ..., p(-N+1,N), ..., p(0,0), ..., p(N,N) \big]^T
\end{aligned}
$$

$$
\boldsymbol{R} = \left[
\begin{array}{ccc}
R(0,0) & \dots & R(0,2N) \\
\vdots & \ddots & \vdots \\
R(0,-2N) & \dots & R(0,0) \\
R(-1,0) & \dots & R(-1,2N) \\
\vdots & & \vdots \\
R(-2N,-2N) & \dots & R(-2N,0)
\end{array}
\right.
$$
$$
\left.
\begin{array}{ccc}
R(1,0) & \dots & R(2N,2N) \\
\vdots & & \vdots \\
R(1,-2N) & \dots & R(2N,0) \\
R(0,0) & \dots & R(2N-1,2N) \\
\vdots & \ddots & \vdots \\
R(-2N+1,-2N) & \dots & R(0,0)
\end{array}
\right]
$$
$$(5)$$

$R(m,n)$ and $p(m,n)$ correspond to the autocorrelation function of $x(i,j)$ and cross-correlation function of $d(i,j)$ and $x(i,j)$, respectively, which are given by

$$R(m,n) = E[x(i,j)x(i-, .j-n)] \qquad (6)$$

$$p(m,n) = E[d(i,j)x(i-m,j-n)] \qquad (7)$$

respectively. However, in practice, the following criterion

$$J = \frac{1}{M^2} \sum_{i=0}^{M-1} \sum_{j=0}^{M-1} \{d(i,j) - y(i,j)\}^2. \qquad (8)$$

is often defined instead of (3) due to its easy computation, and the solution in (4) is obtained. In this case, $R(m,n)$ and $p(m,n)$ are calculated as

$$R(m,n) = \frac{1}{M^2} \sum_{i=0}^{M-1} \sum_{j=0}^{M-1} \{x(i,j)x(i-m,j-n)\} \qquad (9)$$

$$p(m, n) = \frac{1}{M^2} \sum_{i=0}^{M-1} \sum_{j=0}^{M-1} \{d(i,j)x(i-m, j-n)\}$$

$$(10)$$

respectively, from $M \times M$ images of $d(i,j)$ and $x(i,j)$.

The output of the Wiener filter is obtained by (2) with the solution vector in (4).

2.2 Wiener Filter in the Frequency Domain

In the frequency domain, the Wiener filter is given by

$$H(u, v) = \frac{P_D(u, v)}{P_D(u, v) + P_N(u, v)} \qquad (11)$$

where $P_D(u, v)$ and $P_N(u, v)$ represent the power spectra of $d(i,j)$ and $n(i,j)$, respectively. This solution is derived in a similar way with that in the space domain. By minimizing

$$J = E[|D(u, v) - H(u, v)X(u, v)|^2], \qquad (12)$$

where $D(u, v)$ and $X(u, v)$ represent the discrete Fourier transforms (DFTs) of $d(i,j)$ and $x(i,j)$, respectively, the solution is first obtained as

$$H(u, v) = \frac{E[X(u, v)D^*(u, v)]}{E[|X(u, v)|^2]} \qquad (13)$$

where $*$ denotes complex conjugate. When $n(i,j)$ is white noise, the numerator reduces to

$$\begin{aligned} E[X(u, v)D^*(u, v)] &= E[(D(u, v) + N(u, v)) \times \\ & \quad D^*(u, v)] \\ &= E[|D(u, v)|^2] \\ &= P_D(u, v) \end{aligned} \qquad (14)$$

and the denominator reduces to
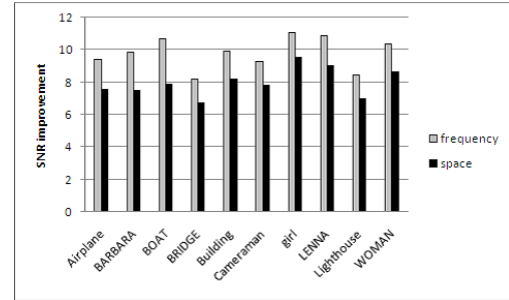
$$E[|X(u, v)|^2] = P_D(u, v) + P_N(u, v) \qquad (15)$$

where $P_D(u, v)$ and $P_N(u, v)$ correspond to the power spectra of $d(i,j)$ and $n(i,j)$, respectively. Thus, (13) results in (11).
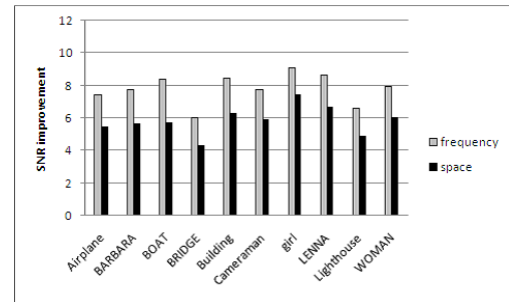
The output of the Wiener filter is given by

$$Y(u, v) = H(u, v)X(u, v) \qquad (16)$$

$$y(i, j) = \text{IDFT}[Y(u, v)]. \qquad (17)$$
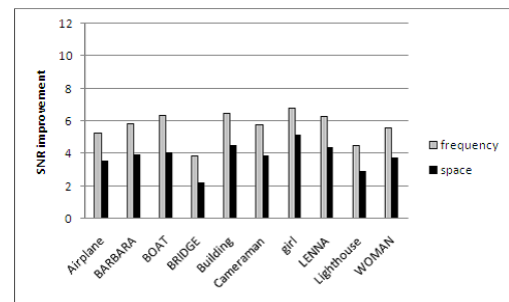
where IDFT in (17) means the Inverse DFT.

(a)SNR=0[dB]

(b)SNR=5[dB]

(c)SNR=10[dB]

Fig. 1: Wiener filtering comparison in space and frequency domains

2.3   Restoration Results in Ideal Case

We investigated the performance of the two types of Wiener filter in an ideal case where the original and noise images are known a priori. We used 10 images in SIDBA, each of which has a size of 256×256 gray scales. A white noise was generated and added to each image, resulting in the preparation of 0[dB] and 5[dB] and 10[dB] noisy images for each image. For each SNR setting, 100 individual white noises were generated and the performance was evaluated as the average of 100 individual runs for each SNR.

The results obtained by each implementation of the two Wiener filters on the degraded images are shown in Figure 1. The window size of the Wiener filter in the space domain was set to 5×5. This is because this setting for the window size is very often used [4]. The SNR improvement was evaluated for comparison. The SNR improvement in [dB] is defined as

$$SNR\ improvement\ [dB]$$
$$= 10 \log_{10} \frac{NMSE[d(i,j), x(i,j)]}{NMSE[d(i,j), y(i,j)]} \quad (18)$$

where

$$NMSE[d(i,j), x(i,j)]$$
$$= 100 \times \frac{Var[d(i,j) - x(i,j)]}{Var[d(i,j)]} \quad (19)$$

$$NMSE[d(i,j), y(i,j)]$$
$$= 100 \times \frac{Var[d(i,j) - y(i,j)]}{Var[d(i,j)]}. \quad (20)$$

Figure 2 shows an example of the restorations obtained by the two Wiener filters in case of SNR=5[dB]. It is obviously observed that much more noise is removed by using the frequency domain Wiener filter in comparing (c) with (d) in Figure 2.

From Figures 1 and 2, we see that the Wiener filter in the frequency domain is more effective than that in the space domain.

3   Power Spectrum Estimation for Wiener Filter

In practice, we cannot obtain the true original image and noise or their power spectrum counterparts that are directly necessary for the Wiener filter design. Therefore, we have to estimate them in order

(a) original   (b) degraded (SNR5[dB])

(c) output of frequency   (d) output of space
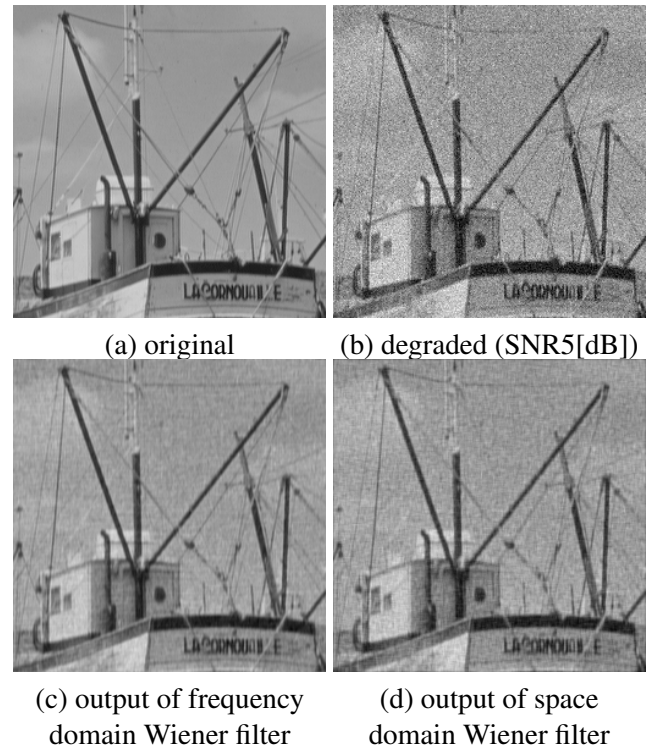domain Wiener filter   domain Wiener filter

Fig. 2: Example of images restored by two Wiener filters

to restore the original image from the degraded image by the Wiener filter. However, there are no reliable techniques which are very suited for power spectrum estimation to design the Wiener filter in the frequency domain. If the noise image, which should be included in the observed noisy image, is obtained in an indirect fashion (in this case, the noise image will not be equivalent to that included in the observed noisy image), then various types of power spectrum estimation are available as shown in [8]. In most of the cases, however, only the observed noisy image is given. Thus, from the noisy image we have to estimate the original image power spectrum as well as the noise power spectrum.

In this section, we present three pairs of the original image and noise power spectrum estimation from the noisy image. The three pairs are derived from the concepts of FBDP [10], modified FBDP and averaging high frequency components (AHFC), respectively.

First we describe a noise estimation method addressed in [10], in which the noise power spectrum is estimated from an image degraded by white noise based on the concept of FBDP. The corresponding method for the original image power spectrum estimation is then derived. As the extension of the FBDP, next, we derive a modified FBDP which provides an improvement in the noise power spectrum estimation. The corresponding original image power spectrum is
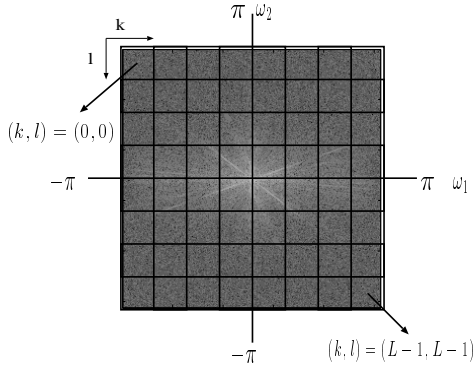
Fig. 3: Blocks in the frequency domain ($L = 8$)

simultaneously obtained in the modified FBDP process. The third approach, AHFC, is a part of the modified FBDP, which is derived as the noise power spectrum estimation method. The corresponding method for the original image power spectrum estimation in this case is then derived.

3.1 FBDP

In general, the power spectrum of an image is concentrated in a low frequency region, while the power spectrum of white noise exists in all frequency regions. Therefore, by restoring a high frequency region of the degraded image, the noise image should be obtained. This is because only the noise components are dominant in a high frequency region of the degraded image. Based on this principle, the following noise estimation method was addressed in [10].

(Step.1) We calculate $X(u, v)$ by the DFT of the input image $x(i, j)$ and obtain its power spectrum and logarithmic power spectrum as $P_X(u, v) =| X(u, v) |^2$ and $G_X(u, v) = \log P_X(u, v)$, respectively.

(Step.2) Dividing $P_X(u, v)$ and $G_X(u, v)$ into $L \times L$ blocks as shown in Figure 3, we obtain $P_{X,(k,l)}(u, v)$ and $G_{X,(k,l)}(u, v)$, respectively, where $P_{X,(k,l)}(u, v)$ and $G_{X,(k,l)}(u, v)$ correspond to the (k, l)-th block of $P_X(u, v)$ and $G_X(u, v)$, respectively. The average of each logarithmic power spectrum $G_{X,(k,l)}(u, v)$, $\bar{G}_{X,(k,l)}(u, v)$, is calculated for each block.

(Step.3) A threshold decision is made for each $\bar{G}_{X,(k,l)}(u, v)$, and $P_X(u, v)$ is divided into its low and high frequency counterparts, $P_{X,low}(u, v)$ and

$P_{X,high}(u, v)$, as

$$P_{X,low}(u, v) = \begin{cases} P_{X,(k,l)}(u, v) & \bar{G}_{X,(k,l)}(u, v) > TH \\ 0 & otherwise \end{cases}$$
(21)

$$P_{X,high}(u, v) = \begin{cases} P_{X,(k,l)}(u, v) & \bar{G}_{X,(k,l)}(u, v) \leq TH \\ 0 & otherwise \end{cases}$$
(22)

$$TH = (G_{X,max} - G_{X,min})/100 * p + G_{X,min} \quad (23)$$

where $G_{X,max}$ and $G_{X,min}$ are the maximum and minimum values of $\bar{G}_X(u, v)$, respectively and p is the division ratio.

(Step.4) The noise components in the degraded image are obtained as its noise power spectrum from the high frequency parts as

$$P_N(u, v) = P_{X,high}(u, v) \quad (24)$$

where $P_N(u, v)$ means an estimate of the noise power spectrum.

This noise power spectrum estimation method was originally proposed for the spectral subtraction method. In implementing the spectral subtraction method, the original image power spectrum is not necessary. In implementing the Wiener filter in the frequency domain, however, the original image power spectrum is definitely required. This is easily accomplished by

$$P_D(u, v) = P_X(u, v) - P_N(u, v) \quad (25)$$

based on the assumption in (1) that the noise is additive to the image. In the FBDP process, (25) is equivalent to

$$P_D(u, v) = P_{X,low}(u, v). \quad (26)$$

When the estimates (24) and (26) are subscribed in (11), the Wiener filter is designed. Equation (26) is recognized as Step 5 of the FBDP method for power spectrum estimation.

Figure 4 shows a block diagram of the FDBP method. A performance example of the method is illustrated in Figure 5.

In [10], the optimal values of parameters L and p were experimentally determined as 32 and 12, respectively, so that the spectral subtraction method provides the best performance. These parameters were used in the FBDP method even for the Wiener filter.

3.2 Modified FBDP

For the noise power spectrum estimation in FBDP, the noise in a low frequency region is not considered. This
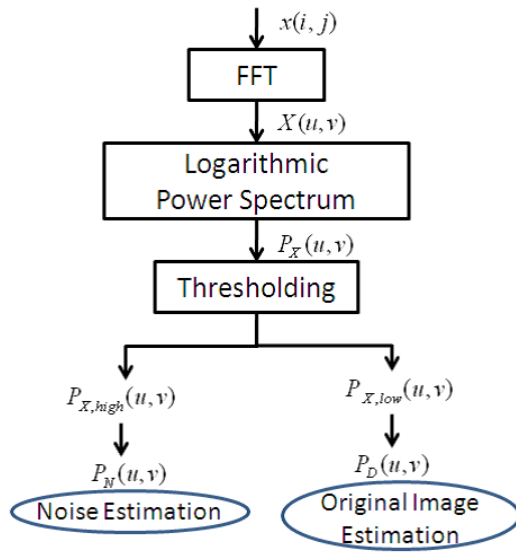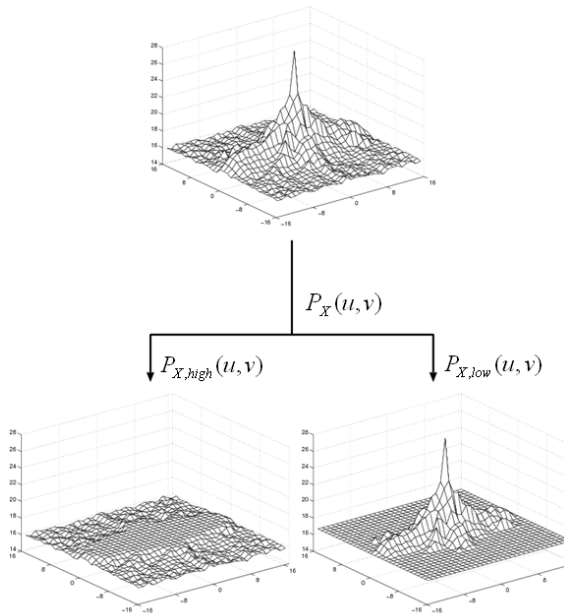
Fig. 4: Block diagram of FBDP

Fig. 5: Power spectra in low and high frequency regions for FBDP method

results in that we can not remove the noise in a low frequency region if we estimate the noise by using the method and restore the degraded image. Therefore, we extend here a method that estimates the noise power spectrum in both low and high frequency regions so that the Wiener filter provides better performance.

The point of the extended noise estimation method is compensation for low frequency regions. Based on (22) in FDBP, the noise power spectrum estimation is modified as

$$
\begin{aligned}
&P_{X,high}(u,v) \\
&= \begin{cases} P_{X,(k,l)}(u,v) & \bar{G}_{X,(k,l)}(u,v) \leq TH \\ \text{average}\big[P_{X,(0,0)}(u,v), P_{X,(0,L-1)}(u,v), \\ P_{X,(L-1,0)}(u,v), P_{X,(L-1,L-1)}(u,v)\big] \\ & otherwise \end{cases}
\end{aligned}
\tag{27}
$$

where average [] represents an averaging operation.

In (27) , the equation for $\bar{G}_{x,(k,l)}(u,v) \leq TH$ is the same as that in (22). The additional part is only the averaging one. This addition comes from the following reasons. The original image has most of the frequency components in a low frequency region. This results in the fact that the high frequency components of the image degraded by white noise are only noise, because the white noise has a flat power spectrum in all the frequency regions. According to this inspection, we set out to cover the low frequency region of the noise power spectrum with average of blocks of four corners being at the highest frequencies. These four corners correspond to those of $L \times L$ blocks in Figure 3. For the modified FBDP, thus, the noise power spectrum estimate is obtained by (24) with $P_{X,high}(u,v)$ in (27).

On the other hand, the original image power spectrum can be simply obtained by (25) again. However, this is not equivalent to (26), when $P_{X,high}(u,v)$ in (27) is used as the noise power spectrum. This is because the low frequency components are included in $P_{X,high}(u,v)$ in (27), while those are not included in $P_{X,high}(u,v)$ in (22). For the modified FBDP, we utilize (26) as the original image power spectrum. This results in better performance of Wiener filtering.

The modified FBDP method consists of 5 Steps as described in the FBDP method. The only different part with the FBDP method is Step 3. For the modified FBDP method, (27) is used instead of (22) in Step 3. The modified FDBP is summarized as shown in Figure 6.

Figure 8 demonstrates the noise power spectrum estimation in the modified FBDP. Power spectra in
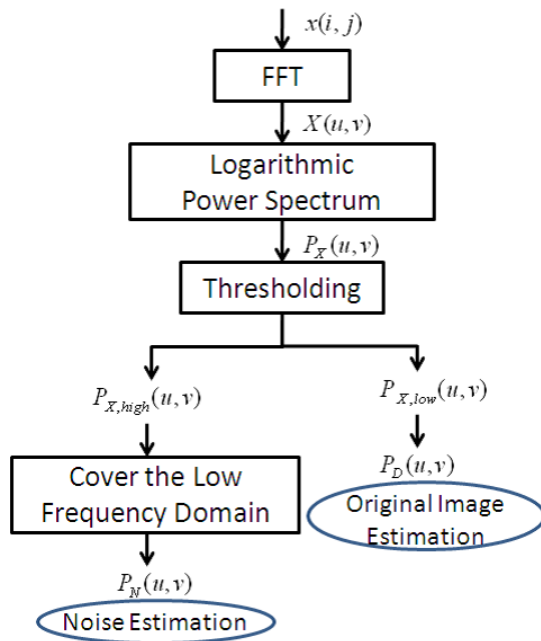
Fig. 6: Block diagram of modified FBDP

(a)noise power spectrum
in FBDP

(b)noise power spectrum
in modified FBDP

Fig. 8: Noise power spectra in FBDP and modified FBDP

Figure 8 were obtained from a noisy Cameraman image in the case of SNR=10 [dB], the power spectrum of which is shown in Figure 7. From Figure 8 it is observed that the low frequency region is compensated by a constant power in the modified FBDP.
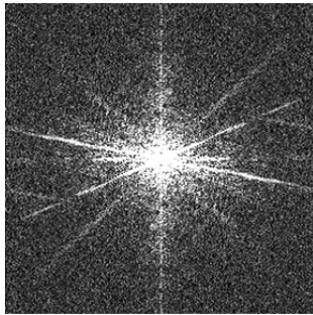

Fig. 7: Power spectrum of Cameraman in case of SNR=10[dB]

It may be necessary for the power spectrum estimation in the modified FBDP to investigate the optimal values of parameters L and p. L is considered not to be influenced by difference between the spectral subtraction method and Wiener filtering, because L corresponds to the block size used for frequency division. Therefore, we supposed that the optimal value of parameter L is 32, which is the same as in [10], and examined only the parameter p dependency.

Figures 9 and 10 show a sensitivity of selection of p. Figure 9 illustrate examples of the noise power

spectra obtained by the modified FBDP in the cases of $p = 10$ and $p = 20$ on a noisy Boat image. Figure 10 corresponds to noise images restored from the frequency components shown in Figure 9. We can observe that larger setting for p results in a noise image that includes the original image.

For images of SNR 0, 5 and 10[dB], the relation between the division rate p and SNR improvement was investigated. The SNR improvement was evaluated for averaging 100 individual white noise generations on each image and further averaging 10 SIDBA images. The results are shown in Figure 11. From Figure 11, we can observe that for near the optimal value of the division rate p providing the highest SNR improvement, there is no great difference in restoration accuracy on most of the images. From the results in Figure 11, we determined $p = 8.5$ for the best setting of the division rate and commonly used this for the modified FBDP method in the Wiener filter design.

3.3 AHFC

From the principle that a white noise has a constant value of power spectrum, the following procedure is straightforward for noise power spectrum estimation. In Step 3 of FBDP, we average blocks of four corners being at the highest frequencies and obtain the noise power spectrum as

$$
\begin{aligned}
P_N(u,v) = \quad & \\
\text{average}\big[& P_{X,(0,0)}(u,v), P_{X,(0,L-1)}(u,v), \\
& P_{X,(L-1,0)}(u,v), P_{X,(L-1,L-1)}(u,v) \big].
\end{aligned}
$$

(28)

In this case, the original image power spectrum is obtained by (25). This technique is called AHFC in this paper.

(a)$p = 10$ (b)$p = 20$
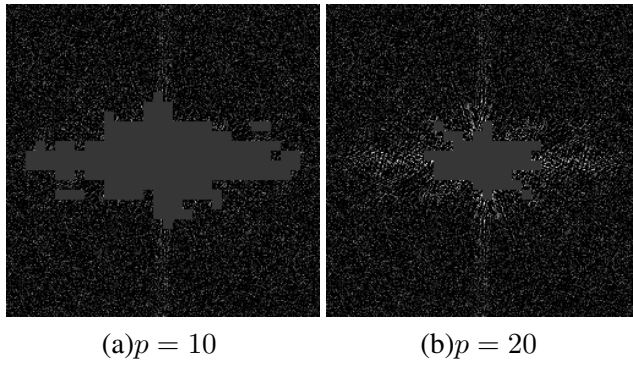
Fig. 9: Noise power spectra obtained from noisy Boat image in case of SNR=5[dB]

(a) SNR=0[dB]

(b) SNR=5[dB]

(c) SNR=10[dB]

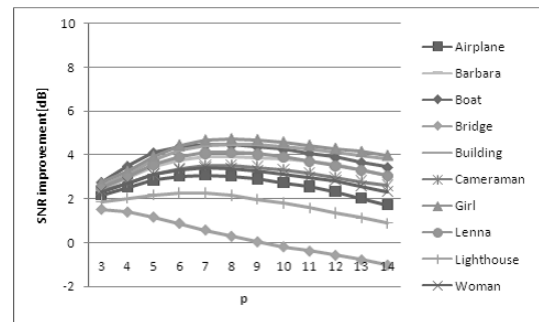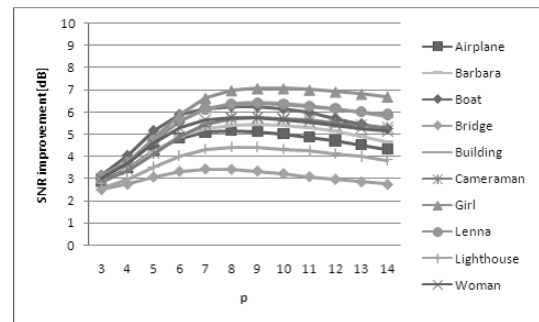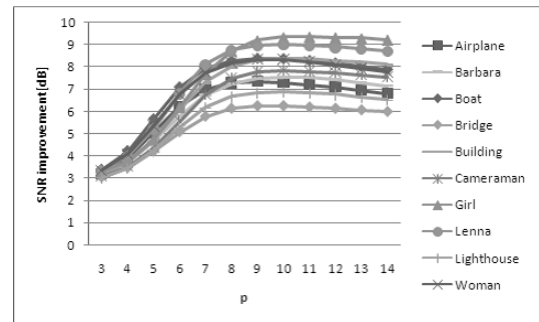(a)$p = 10$ (b)$p = 20$
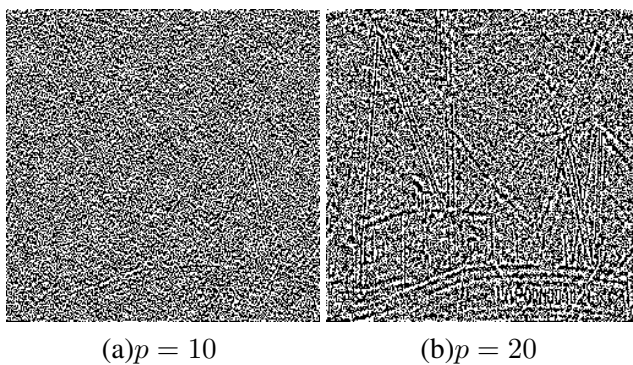
Fig. 11: Relation between p and SNR improvement.

Fig. 10: Noise images obtained from noisy Boat image in case of SNR=5[dB]

The AHFC method consists of 4 Steps. Steps 1 and 2 are common with those of FBDP. Step 3 is (28) and Step 4 is (25).

4   Comparison of Restoration

In this section, the performances of the Wiener filter with FBDP, modified FBDP (MFBDP) and AHFC are compared.

We used 10 images in SIDBA. We added a white noise to each image and prepared noisy images of 0[dB] and 5[dB] and 10[dB] for each image. Also, for each SNR setting, 100 individual white noises were generated and investigated. Each score is an evaluation of averaging on these 100 images for each SNR setting.

In addition to SNR improvement, we deployed achievement ratio (AR) defined as [SNR improvement in real environment] / [SNR improvement in ideal environment] for assessment. The value of 1.0 for AR indicates 100 percent achievement.

Figure 12 shows a performance comparison in SNR improvement. From Figure 12, it is commonly observed that the modified FBDP provides the best performance regardless to SNR. The FBDP is better than the AHFC in low SNR cases, while the AHFC is better in some cases of high SNR.

Figure 13 is a performance comparison in AR. Similar results with those in Figure 12 are observed.

Figures 14, 15 and 16 show examples of restorations from noisy Barbara images of SNR=0, 5, and 10 [dB], respectively. Restoration in an ideal case where the original and noise power spectra are known a priori corresponds to (c) ideal. From Figures 14, 15 and 16 it is observed that images restored by AHFC includes comparatively larger amount of noise. The amount of noise included in images restored by FBDP are less, but severe blurs are observed. Features of images restored by modified FBDP are less noise and less blurs.

5   Concluding Remarks

In this paper, we have investigated the Wiener filter for restoration from an image degraded by white noise. In an ideal case where both the original and noise images are known, it has been found that the Wiener filter in the frequency domain is more effective than that in the space domain. In order to apply the frequency domain Wiener filter in real cases, we need estimates of the original and noise power spectra. To this end, we have investigated three methods; FBDP, modified FBDP and AHFC. Examining the performance of the
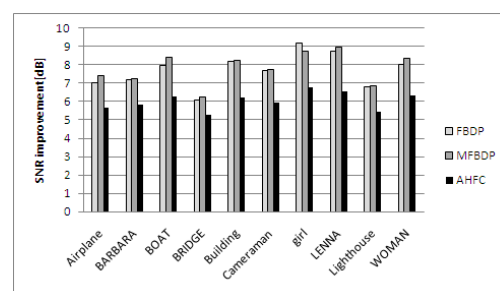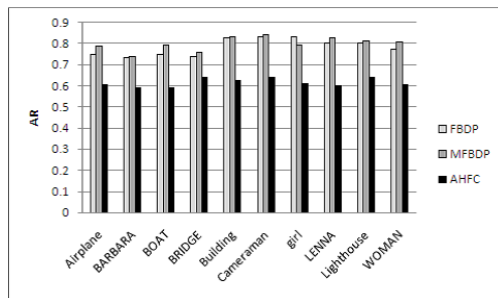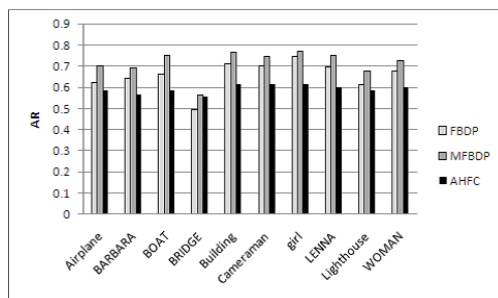

(a)SNR=0[dB]
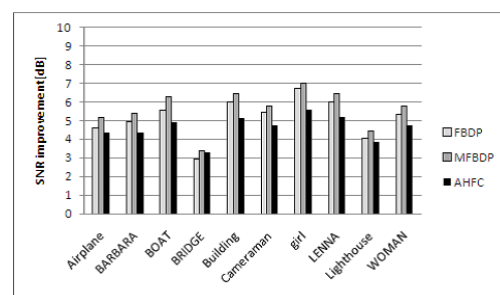
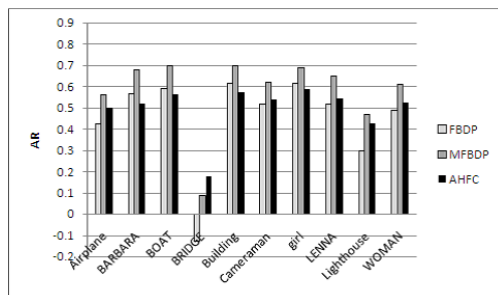(b)SNR=5[dB]
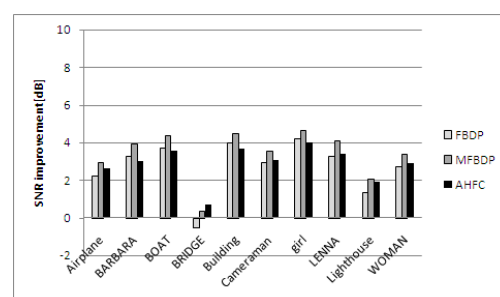
(c)SNR=10[dB]

Fig. 12: Comparison in SNR improvement

(a)SNR=0[dB]

(b)SNR=5[dB]

(c)SNR=10[dB]

Fig. 13: Comparison in AR

(a) original   (b) degraded

(c) ideal   (d) AHFC

(e) FBDP   (f) MFBDP

Fig. 14: Image restoration of Barbara in case of SNR=0[dB]

frequency domain Wiener filter by using these power spectrum estimation methods, we have confirmed that the modified version of FBDP brings the best performance with reducing noise and blurring in the processed image.

References:

[1] P. Bojarczak and S. Osowski, Denoising of Images - A Comparison of Different Filtering Approaches, *WSEAS Trans. Computers*, Issue 3, Vol.3, pp.738-743, July 2004.

[2] A. Khare and U. S. Tiwary, Symmetric Daubechies Complex Wavelet Transform and Its Application to Denoising and Deblurring, *WSEAS Trans. Signal Processing*, Issue 5, Vol.2, pp.738-745, May 2006.

[3] V. Niola and G. Quaremba, Evaluation of Image Denoising Using Fuzziness Measures, *WSEAS Trans. Systems*, Issue 7, Vol.5, pp.1548-1554, July 2006.
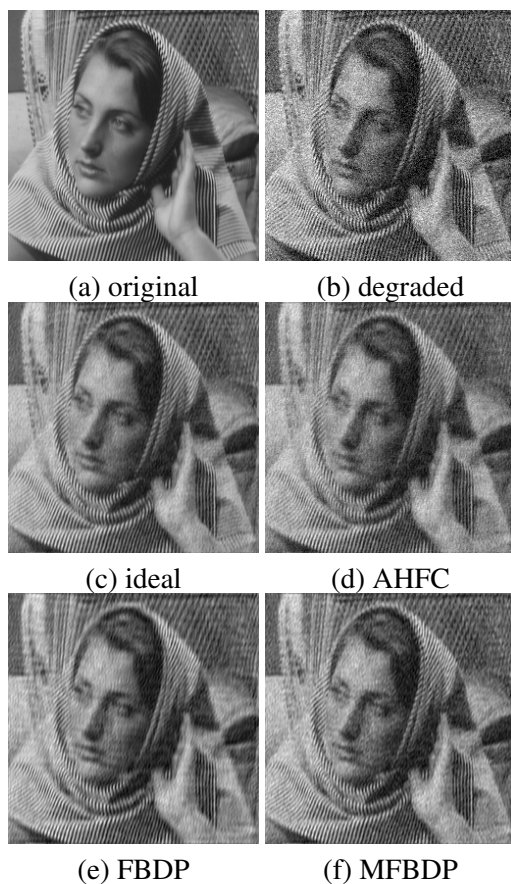
(a) original   (b) degraded

(c) ideal   (d) AHFC

(e) FBDP   (f) MFBDP

Fig. 15: Image restoration of Barbara in case of SNR=5[dB]

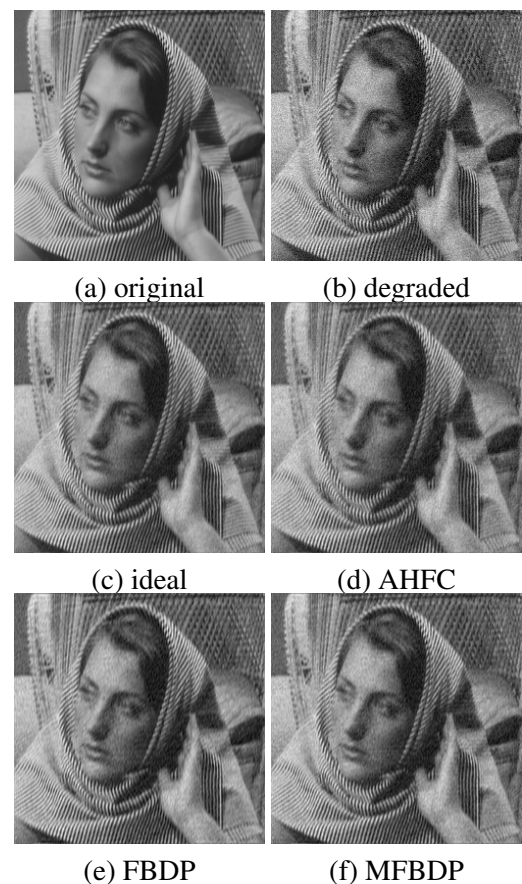(a) original   (b) degraded

(c) ideal   (d) AHFC

(e) FBDP   (f) MFBDP

Fig. 16: Image restoration of Barbara in case of SNR=10[dB]

[4] M.Muneyasu and A.Taguchi, *Nonlinear Digital Signal Processing*, Asakura Shoten, 1999 (in Japanese).

[5] G. R. Arce, *Nonlinear Signal Processing : A Statistical Approach*, Wiley, 2005.

[6] G. Strang and T. Nguyen, *Wavelet and Filter Banks*, Wellesley-Cambridge Press, 1997.

[7] I. T. Young and J. J. Gerbrands and L. J. Van Vliet, *Fundamentals of Image Processing*, ISBN 90-75691-01-7, 1998.

[8] J. S. Lim, *Two-Dimensional Signal and Image Processing*, Prentice Hall, 1990.

[9] H. C. Andrews and B. R. Hunt, *Digital Image Restoration*, Prentice Hall, 1990.

[10] T. Kobayashi, T. Shimamura, T. Hosoya and Y. Takahashi, Restoration from Image Degraded by White Noise Based on Iterative Spectral Subtraction Method, *Proceedings of IEEE International Symposium on Circuits and Systems*, pp.6268-6271, 2005.